Determination of the natural frequencies of ultralight carbon fiber trusses for silicon tracking systems

M. Herrera

Veksler and Baldin Laboratory of High Energy Physics, Joint Institute for Nuclear Research, Dubna, Russia. & Facultad de Ciencias, Universidad de Colima, Bernal Díaz del Castillo No. 340, Col. Villas San Sebastián, Colima 28045, México.

T. Ligdenova, C. Ceballos and D. Dementev

Veksler and Baldin Laboratory of High Energy Physics, Joint Institute for Nuclear Research, Dubna, Russia.

S. Igolkin and V. Zherebchevsky

Saint Petersburg State University, Saint Petersburg, Russia.

Received 14 May 2024; accepted 25 June 2024

In this work a method is developed to determine the natural frequency of highly-irradiated ultralight carbon fiber trusses. This method is based both in experimental acoustic measurements and the ANSYS-based modeling of the trusses. The structures under study are sensor supporting trusses widely used in silicon inner trackers of large experimental setups at LHC, FAIR and NICA.

Keywords: Silicon inner trackers mechanics; sensor support trusses; natural frequency.

DOI: https://doi.org/10.31349/RevMexFis.70.060902

1. Introduction

The development of the Nuclotron-based Ion Collider fAcility (NICA) currently underway at the Joint Institute for Nuclear Research (JINR) includes large experimental setups like the MPD [1], SPD [2], and BM@N [3] which incorporates silicon tracking systems to trace thousands of charged secondary particles produced in hadron- and nucleus-nucleus high energy collisions. Existing, and soon to appear, modern silicon sensors are available in monolithic or non-monolithic versions of the readout frontend electronics providing excellent spatial (5 μm) and time resolution (40 ps). However, the performance of the final setup might be degraded due to resonant oscillations of the large-area and low material budget supporting structures that usually carry together thousands of relatively small active sensor elements induced by the vibration of external elements like the cooling and vacuum systems pumps, when coinciding with the structures' natural frequency. The potential hazard due to vibration-related degradation of the spatial resolution of ultralight supporting structures seems to grow following the existing plans of using such mechanical structures in experiments with increased luminosity at HL-LHC [4], FAIR [5] and others to follow. In years past the major material for building the mechanical supporting structures of the existing silicon tracking systems was high-Young's-modulus carbon threads laminated together in epoxies. Polymerization of those manufactured carbon fiber joins together thousands of individual carbon threads in the element of the supporting structure. It is known that mechanical properties of epoxy degrade under radiation. Therefore, a question of what will happen to the supporting trusses of a tracker in high luminosity experiments after expected 10 years fluencies of secondary hadrons up to values of 10^{16} seems to be timely and relevant before such trackers are to be built or existing ones to be still engaged.

The technology for manufacturing ultra-light carbon fiber sensor supporting trusses was initially developed for the Inner Tracking System of ALICE at the Saint Petersburg State University, Russia [6]. Later on, it was also used for producing the supporting structures of the new MAPS-based Inner Tracking System (ITS2) for the ALICE upgrade [7, 8] operating at the LHC since 2023 with plans to prolong lifetime of the system after LHC substantial luminosity increase scheduled for 2029 [9]. The same technology for manufacturing trusses with slightly different geometry form factors was also used at JINR for production of sensor supports for the Silicon Tracking System (STS) of the CBM experiment at FAIR [5] and upgraded BM@N experiment at NICA [3].

Potential degradation of mechanical properties of the key elements of the tracker, namely the sensor supporting ultralight carbon trusses ("spaceforms"), may cause not only systematic displacement of the sensors attached to frames but, what is more hazardous, badly impact the spatial resolution of the system due to appearance of resonance vibrations of the trusses. To address this issue, we plan to perform a mechanical characterization of sensor supporting trusses currently in use by the ALICE ITS2 tracker laminated with different types of adhesives by means of determining their natural frequency before and after being irradiated at JINR IBR2 facility [10]. Since after irradiations the trusses will be radioactive all post irradiation manipulation with the tested subjects should be performed remotely. This work describes

the results of the development of a method proposed by us for purpose to determined of the first natural frequency of the trusses based on direct acoustic-based measurements as well as their modeling in the framework of the ANSYS code.

2. Materials and methods

The main idea of the work was to compare the results of experimental and simulated determinations of normal frequency spectra of a truss of the kind used in silicon trackers in order to crosscheck these results as a validation of a direct yet remote method for the determination of the natural frequency of of activated trusses that would not require an extensive manipulation of them.

The selected type of truss for the determination of its natural frequency was of the kind used as supporting structure of the sensor elements in ALICE ITS2 Outer Barrel at CERN that will be also used in NICA's MPD-ITS detector at JINR (Fig. 1). It comprises a carbon fiber structure with a length of 1526 mm and a triangular cross section produced in simultaneous punch-and-mold lamination of three long beams having corner-like shape together with a set multiple thin cylindrical ribs connecting the beams of a truss together at angle of 45°.

The natural frequency of the unloaded truss free from external influences was experimentally determined by the acoustic-based experiment schematically represented in Fig. 2. The setup is composed by the truss under test (1), a truss vibration exciter capable of variable frequency oscillations (2), eddy-current probe ZET 701 vortex sensor (3), a driver facilitating connection to a PC (4), and an electric conductive plate (5). In order to minimize external disturbances, the setup was mounted on a robust laser table. The amplitude of the oscillations was measured based on a contactless vortex sensor covering a frequency range from 30 to 300 Hz. This sensor has an inductance coil at the tip of the probe generating an alternating electromagnetic field, inducing eddy currents in the test object, and subsequently altering coil parameters based on the gap between the sensor's end and the controlled object, allowing to measure the distance to the object over time. The resulting electrical signal undergoes linearization and scaling by the driver.

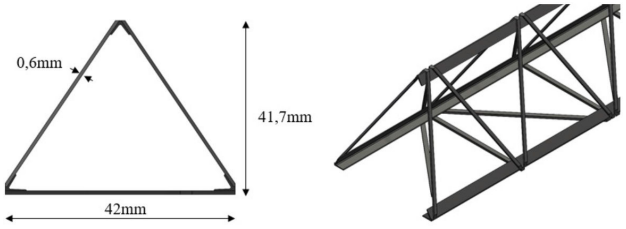

FIGURE 1. Support truss of Inner Tracking System of the MPD experiment.

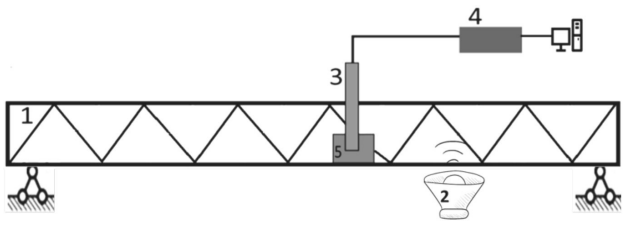

FIGURE 2. Layout of direct experiment for study of the natural frequency spectrum of a truss. 1- truss under test; 2- truss vibration exciter of variable frequency oscillations; 3- vortex sensor probe; 4- driver for connecting the probe to a PC; 5- electric conductive plate.

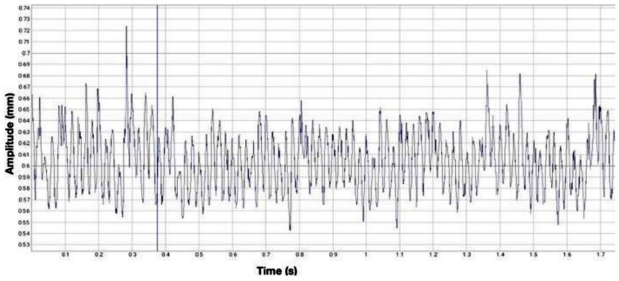

FIGURE 3. Measured signal as a function of time of the gap between the vortex sensor and the conductive plate for the MPD-ITS truss for an exciter's frequency of 50 Hz.

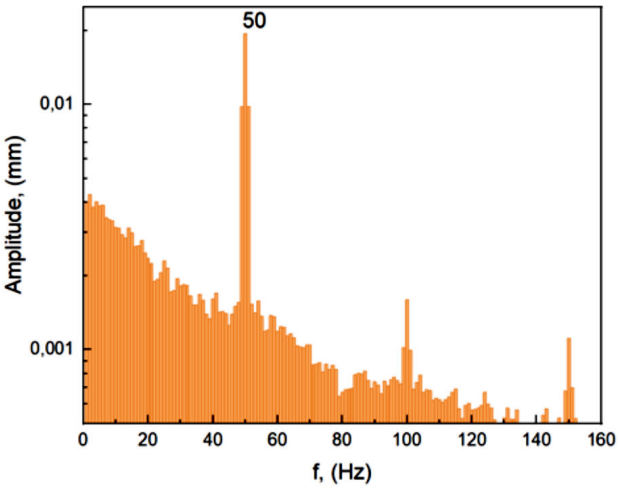

FIGURE 4. Resulting spectrum after applying the Fourier transform to the signal from Fig. 3.

For determining the value of the natural frequency, the exciter's frequency was varied from 30 Hz to 300 Hz. At each step the variation of the gap between the vortex sensor and the conductive plate was recorded during 20 s with a sampling rate 1 kHz as it is shown in Fig. 3 for the first 2 s and a frequency of the exciter of 50 Hz. Afterwards, the obtained signal was converted into a frequency spectrum by means of the Fourier transform (Fig. 4). The amplitude of the oscillation for the selected frequency was determined as a standard deviation of the measured gap values for the recorded time period. The same process was repeated for the next frequency. All the obtained oscillation amplitudes were plotted as the function of the exciter's frequency as shown in Fig. 7 in the next section (experimental values) and the natural fre-

TABLE I. Average of the meassured sagging values of the trusses for different mass loads.

Mass load (gr)	Sagging (mm)
50	0.07±0.01
100	0.12±0.01
150	0.18±0.01
200	0.24±0.01

quency of the truss was determined from the first peak of the plot (first natural frequency). Initially the frequency of the exciter was varied with a step of 10 Hz and once the peak position was identified the corresponding region was re-scanned with a step of 1 Hz.

On the other hand, the natural frequency of the trusses was independently determined from the data included on the datasheet regarding measurements of sagging values for different mass loads (m_L) applied on top of the center of the truss as shown in Table I where the reported sagging for each mass load is the average value from a sample of 30 trusses.

For this, despite its composite structure of the trusses the system was approximated in first order to a uniform beam with a mass *P* load placed in the center resulting in a sagging *u* that according to the Castigliano's theorem [11, 12] is defined as

$$u = \frac{PL^3}{48EI}, \tag{1}$$

where *E* is the modulus of elasticity of the beam and *I* the moment of inertia.

Subsequently the sagging is substituted by an analog system [13] where a load of mass m_L is suspended from a spring of stiffness *k* placed at the center of the truss for which the natural frequency can be expressed as

$$f_n = \frac{1}{2\pi}\sqrt{\frac{m_L g}{\delta_t m_t}}, \tag{2}$$

where m_t is the mass of the truss and

$$k = \frac{m_L g}{\delta_t}, \tag{3}$$

where δ_t is the sagging of the truss. Since $\delta_t = u$, it is possible to approximate the natural frequency value of the real truss without knowing the mechanical properties of the material, because the result of the sagging is implicitly included in the modulus of elasticity and inertia moment, as shown in Eq. (1). The value of the natural frequency of the loaded truss was determined by linearly fitting the sagging values from Table II as a function of the corresponding mass load using Eq. (2) in the form

$$\delta_t = \frac{g}{4\pi^2 m_t f_n^2} m_L \tag{4}$$

as it is shown in Fig. 5, resulting in f_n = 74.41±1.46 Hz.

Additionally, a model of the truss was created in ANSYS and a simulation of its sagging under mass loads was carried out in ANSYS Structural Static module by means of the finite

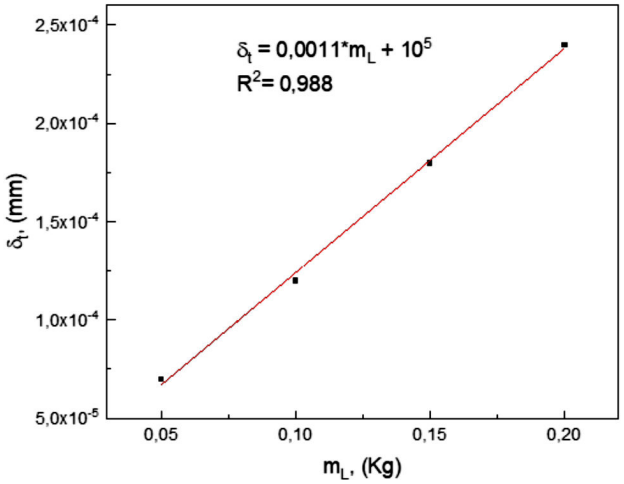

FIGURE 5. Linear fit of the sagging values from Table I as a function of the corresponding mass load.

element method. MPD-ITS trusses are constructed using two types of materials: fiber M55J impregnated with an epoxy binder for the ribs of the frame and prepreg consisting of M55J for the longitudinal beams. The technical datasheet for M55J only includes information on the Modulus of Elasticity in the direction along the fibers, while the Poisson modulus and Shear modulus are unspecified. As so, the material of the trusses was modeled as isotropic using the properties for Prepreg and M55J from ANSYS library (Table II) with a density of 1933 Kg/m^3 , calculated from the truss' volume that was determined using ANSYS-SpaceClaim. Then the value of the modulus of elasticity was varied for a given mass load until a sagging value as close as possible to the value reported in the experimental data was obtained. As a counter check the corresponding natural frequency obtained in ANSYS for such material composition of the truss under mass load was compared with the results obtained from the calculations using Eq. (2).

Once the Modulus of Elasticity was set it was used along with the already established isotropic material composition for modelling into ANSYS the unloaded truss for the determination of its natural and the result was compared with the frequency obtained from the acoustic experiment. Finally, unloaded trusses of different lengths were modeled in ANSYS using the previously obtained composition and the corresponding natural frequencies obtained from the ANSYS modal analysis module were compared with the experimental values obtained from acoustic measurements for the same set of lengths measured at different fixed positions along the truss frame; 1526 mm, 1290 mm and 1030 mm.

TABLE II. Isotropic M55J material properties from ANSYS library.

Property	Value
Modulus of Elasticity	300 GPA
Tensile Yield Strength	186 GPA
Compressive Ultimate Strength	835 MPA

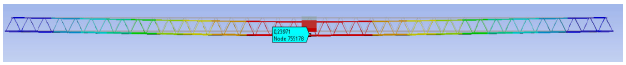

FIGURE 6. Sagging of the ITS space frame (mm), isotropic material, load 200 gr, magnified by a factor of x50.

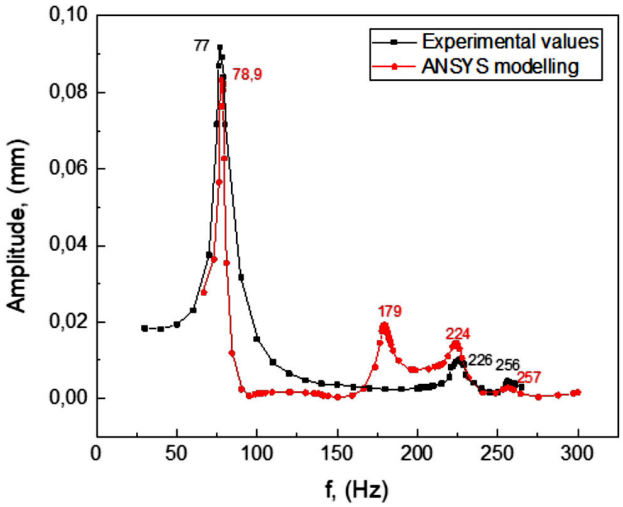

FIGURE 7. Experimental values and simulated ones (considering an isotropic material composition) of the natural frequency of the unloaded MPD-ITS truss.

TABLE III. Simulation results using different materials with proposed isotropic properties for MPD-ITS truss for a load of 200 g.

Modulus of Elasticity (GPa)	Sagging (mm)	f_n (Hz)
300.0	0.099	115.14
135.0	0.219	77.244
133.0	0.229	76.654
128.9	0.239	73.669
100.0	0.293	66.475

3. Results

By means of the narrow band spectral analysis of the gap between the vortex sensor and the conductive plate based on the Fourier transform described in the previous section the first natural frequency of the unloaded MPD-ITS trusses was experimentally determined to be 77 ± 0.55 Hz, as it is shown in Fig. 7 (experimental values).

On the other hand, Table III shows the values of the resulting sagging obtained in the ANSYS model of the MPD-ITS truss for different isotropic materials of density 1933 Kg/m^3 by varying the value of the modulus of elasticity for a load of 200 g placed in the center of the structure as shown in Fig. 6, where the sagging has been magnified by a factor 50 for visual purposes.

From these results the modulus of elasticity for the truss material was set to 128.9 ± 0.1 GPa for being the value for which the resulting sagging was closer to the reference value

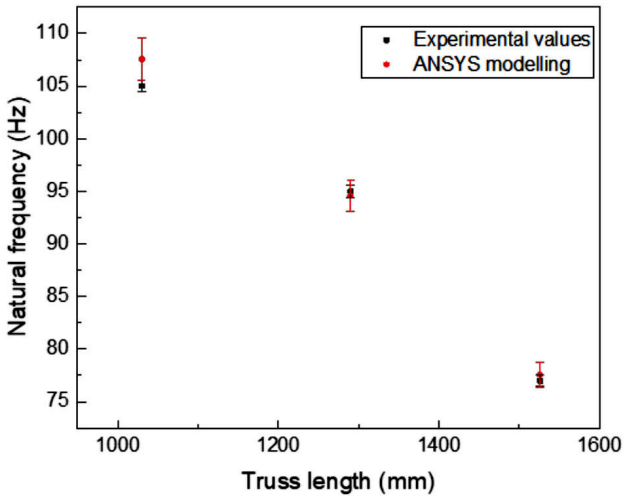

FIGURE 8. Dependence of the natural frequency on the length of unloaded MPD-ITS trusses.

of 0.24 mm reported in Table I. As it can be seen, the corresponding natural frequency in that case is 73.7 ± 1.44 Hz, which differs by 0.9% from the value of 74.41 ± 1.46 Hz obtained from the calculations based on the datasheets data of the trusses.

Using the established material properties the natural frequency of the unloaded truss was then determined in the ANSYS model and compared with the experimental value obtained from the acoustic experiment as shown in Fig. 7.

It can be seen that when the truss is unloaded the value of the first natural frequency from the simulation is 78.9 ± 1.21 Hz while the experimental value is 77 ± 0.55 Hz, so there is a difference of 2.5% between the two methods.

The result of the determination of the natural frequency of unloaded trusses of different length is presented in Fig. 8. The lengths were obtained by fixing the truss by means of thermal glue at lengths of 1030 mm, 1290 mm and 1526 mm. The divergence between the values from the simulation and the experiment, as well as the error from the modelling increases as the length of the truss decreases due to the influence of the part of the truss structure lying beyond the fixators in the experiment.

4. Conclusions

The possibility of measuring the natural frequency of the ultra-light mechanical structures used as support of the tracking sensors in large experimental setups like NICA's MPD experiment by means of an acoustic-based experimental setup has been assessed. This setup allows us to perform these measurements in highly irradiated trusses while staying at a safety distance from them. The experimental results were compared with the results from the simulations based on the finite element method using the ANSYS code for modeling the structures under study by approximating its composition

to an isotropic material with equivalent mechanical characteristics as the real ones. In these conditions the discrepancy between the experimental and simulated results was 2.5%.

Aknowledgments

We are grateful to Dr.Yuri Murin for his proposal to carry out this study and his constant interest to its results. Our special thanks are addressed also to our colleague Mikhail Shitenkov who helped us to build and tune the acoustic test bench used in this study. Support for this work was received in part from UNAM-PAPIIT grant number IG100322 and from CONACYT grant numbers CF-2023-G-433 and A1-S-7655.

1. Kh. U. Abraamyan, The MPD detector at the NICA heavy-ion collider at JINR, *NIM A* **628** (2011) 99, https://doi.org/10.1016/j.nima.2010.06.293.
2. I. Savin *et al.*, Spin physics experiments at NICA-SPD with polarized proton and deuteron beams, *Eur. Phys. J. A* **52** (2016) 215, https://doi.org/10.1140/epja/i2016-16215-x
3. P. Senger *et al.*, Upgrading the Baryonic Matter at the Nuclotron Experiment at NICA for Studies of Dense Nuclear Matter, *Particles* **2** (2019) 481, https://doi.org/10.3390/particles2040029
4. I. Bejar Alonso *et al*., High-Luminosity Large Hadron Collider (HL-LHC): Technical design report, *CERN Yellow Reports: Monographs* **10** (2020) 390, https://dx.doi.org/10.23731/CYRM-2020-0010.
5. J. Heuser *et al*., Technical Design Report for the CBM Silicon Tracking System (STS), GSI Report 2013-4 (2013), https://repository.gsi.de/record/54798.
6. N. Ahmad *et al*., (ALICE Collaboration), ALICE: Technical proposal for a Large Ion collider Experiment at the CERN LHC, CERN/LHCC/P3 (1995), https://cds.cern.ch/record/293391.
7. V. I. Zherebchevsky *et al.*, Experimental investigation of new ultra-lightweight support and cooling structures for the new Inner Tracking System of the ALICE Detector, *JINST* **13** (2018) T08003, https://dx.doi.org/10.1088/1748-0221/13/08/T08003.
8. B. Abelev *et al.*, (ALICE Collaboration), Technical Design Report for the Upgrade of the ALICE Inner Tracking System, *J. Phys. G: Nucl. Part. Phys*. **41** (2014) 087002, https://dx.doi.org/10.1088/0954-3899/41/8/087002.
9. The HL-LHC project https://hilumilhc.web.cern.ch/content/hl-lhc-project.
10. IBR-2 User Club, https://ibr-2.jinr.ru/
11. S. Timoshenko, Strength of Materials, Part 1: Elementary Theory and Problems, 2nd ed. (D. Van Nostrand Company, INC., New York, NY, 1940), pp. 143-165.
12. Richard G. Budynas, A. M. Sadegh, Roark's Formulas for Stress and Strain, 9th ed. (McGraw-Hill, New York, NY, 2020), pp. 190-192.
13. A. Chopra, Dynamics of Structures, 3rd ed. (Prentice Hall, Hoboken, NJ, 1993), pp. 41-43.